DOI: https://doi.org/10.54966/jreen.v28i1.1346

Journal of Renewable Energies

Revue des Energies Renouvelables

journal home page: https://revue.cder.dz/index.php/rer

Conference paper

Prediction Cell Parameter of A_2MX_6 Cubic Perovskites

Hadda Krarcha [a,b,c,*], **Abdelhak Ferroudj** [d]

[a] *LRPRIM Laboratory, Dept of Physics, Faculty of Material Sciences, University Batna1, Algeria*
[b] *LPG, laboratory, university 8mai 1945, Guelma, 24000, Algeria*
[c] *Earth Science & Universe Institut University Mosteph Ben Boulaid Batna2, Batna,, Algeria*
[d] *Dept of Physics, Faculty of Material Sciences, University Batna1, Algeria*

ARTICLE INFO

Article history:
Received January 16, 2025
Accepted February 02, 2025

Keywords:
Cell parameter prediction,
Perovskite,
A_2MX_6.

ABSTRACT

A_2MX_6 Perovskite materials have shown impressive advances in the last 50 years due to their photovoltaic application, making them one of the most promising technologies for next-generation solar cells. We present in this work a semi-empirical model for the prediction of cell parameters of cubic A_2MX_6 perovskites. It is useful for providing the predicted structural information for estimating the physical properties of materials for which accurate structural data are not available. We propose a linear formula according to the factors: Interatomic distance $R_A + R_X$ and $R_M + R_X$ and electronegativity difference $\chi_X - \chi_M$. The interatomic distances d_{X-X} and $d_{M-X}d$ can be estimated from the crystalline structure of the compounds studied. A new prediction of cell parameter is estimated for 90 perovskites and the results are compared with the experimental one whose error is of the order of 1.13%.

1. INTRODUCTION

Research on perovskite materials continues to grow year by year. The results obtained in this field have led to major developments, particularly in the photovoltaic field and various technical fields such as telecommunications and computing (resonators, capacitors, memories), or in various applications of electronics (capacitors high performance, insulators, and semiconductors) (C. Kalaiselvi et al. 2018, W. S. Yang et al. 2017, A. Kojima et al. 2009, A. E. Maughan et al. 2016), these materials are also useful for their piezoelectric properties (shock and acceleration sensor, sonar, loudspeaker ...).

The importance of perovskite materials A_2MX_6 is also in the possibility of changing the atomic constituents A, M, and X according to the desired applications.

---

[*] *Corresponding author, E-mail address: krarcha1974@gmail.com*
Tel : + 213 661583317

ISSN: 1112-2242 / EISSN: 2716-8247

The structural stability of the materials is linked to the knowledge of their crystalline structure, especially the cell parameters CP.

The determination of the CP is of great importance in determining the identity of the material. This type of prediction of CP minimizes the cost and time for experimental researchers or simulators. The paper is organized as follows: in section 2, we present a detailed history of different prediction models. Section 3 is divided into two parts: Application of Brik's model and in the second part new reformulation of Jiang's model with comparison and discussion of results. A new reformulation of Jiang's model is adapted for the cell parameter (CP) prediction of this family series. Finally, the conclusion is given in section 4.

2. HISTORICAL OVERVIEW OF CELL PARAMETER PREDICTION MODEL'S

Several models of CP prediction have been developed during the last decades, especially for cubic perovskite structures of types ABX_3 (Fukunaga et al. 1973; Chonghe et al. 2003; Lufaso et al. 2001; Lufaso et al. 2002; Jiang et al. 2006; Feng et al. 2008, Kumar et al. 2008; Moreira et al. 2007; Majid et al. 2010) and even double perovskite of type $A_2XX'B_6$. We first present a historical overview of different prediction cell models.

2.1 Osamu Fukunaga model's 1972

The ternary oxides of the ideal perovskite type took on great importance at that time. The first works of prediction of structural parameters of perovskites ABO_3 are those of Fukunaga et al. (1973).

This model is based on a linear empirical relationship between the cell size and the ionic radius of the ternary components $A^{+2}B^{+4}O_3$ with A = Ba, Pb, Sr, Ca, and Cd. B = Zr, Hf, Sn, and Ti. It started by presenting unit cell size as:

$$V^{1/3}=2R_{B-X} \tag{1}$$

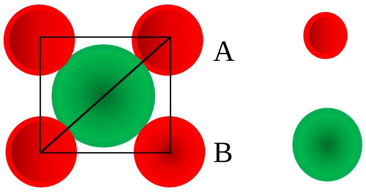

Fig 1. A and B atoms on the (100) plane of cubic perovskite.

Were $R_{B-X} = r_B + r_X$.
Initially, Fukunaga et al. (1973) offered two forms for the tolerance factors s and s':

$$S = \frac{\sqrt{2}[r_B+r_X]}{[r_A^{XII}+r_X]} \tag{2}$$

$$S' = \frac{\sqrt{2}[r_B+r_X]}{[r_A^{VIII}+r_X]} \tag{3}$$

S and S' introduce the coordination number CN effect, considering 8 for the anions A and 12 for cations B. By drawing the curve: of $V^{1/3}$ as a function of R_{B-X} and S we can obtain a linear relation:

$$V^{1/3} = V_0^{1/3} - d(s-1) \tag{4}$$

This formula was checked for 20 materials between oxides, hydrides, and chlorides. This allowed him to rephrase another empirical relationship:

$$V^{1/3} = 2[mr_B + nr_X] - d(S-1) \tag{5}$$

With constant values for each type of anion X

Equation (2) is rewritten as :

$$V^{1/3} = ar_B + b \tag{6}$$

with

$$a = 2m - \sqrt{2}\left(\frac{d}{R_{A-X}}\right) \tag{7}$$

$$b = 2nr_X - \sqrt{2} - \left(\frac{dr_X}{R_{A-X}}\right) \tag{8}$$

The final empirical formulas after adjustment are given by:

$$V^{1/3} = 2.37r_B + 2.47 - 2(S-1). \tag{9}$$

2.2 Structure Prediction Diagnostic Sofware of Michael W. Lufaso (1997-2001)

The SPuDS program (Structure Prediction Diagnostic Sofware) of Lufaso (2001; 2002) is a prediction program for the crystalline structure of perovskites including all possibilities of octahedron BX_6 distortions. This program uses compound inputs to calculate the optimal structure for different Glazer systems (Feng et al. 2008).

2.3 Linear regression method of Li Chonghe 2003

Chonghe et al (2003) are interested in the CP of the $GdFeO_3$ type perovskites that are correlated with the properties of their elemental constituents using a linear regression method LR. Firstly, the LR model was based only on the ionic radius of the constituents A and B, then it was developed to take into account 5 other properties: ionic radius, the electronegativity of the cations A and B, the ion valence that has diminished the error at less than 2%. The Gibbs energy gives accurate information on the equilibrium of a crystal. The network parameter corresponding to this equilibrium energy can be described as a parameter function:

$$A=f(Z_A, Z_B, Z_O, r_A, r_B, r_O, \chi_A, \chi_B, \chi_O) . \tag{10}$$

Z: valence
χ: electronegativity
r: ionic radius.

Oxygen variables are ignored since they are unchangeable for all compounds.

This model allowed the prediction of the CP for different perovskite structures: Rhombohedral, orthorhombic, tetragonal, and cubic by linear regression LR method. For example, tetragonal parameters a and b are given by:

$$a = 17.2443 + 7.5013\ r_A - 3.2537\ r_B - 17.4019.t - 2.1508(r_A/t). \tag{11}$$

$$b = -\ 2.9248 - 0.1803\ r_A + 8.2772\ r_B + 10.7858\ t - 28652\ (r_A/t\ ). \tag{12}$$

with *t* is the Goldsmith tolerance factor.

2.4 Empiric prediction model of L. Q. Jiang (2008)

Most of the compounds have cubic structures of the type $CaTiO_3$ where the size of atom *A* is greater than that of atom *B* (Jiang et al. 2006; Feng et al. 2008)). The cubic structure Pm3m is composed of three-dimensional octahedra BX_6. Atom *A* is surrounded by 12 X anions, as shown in Figure (2).

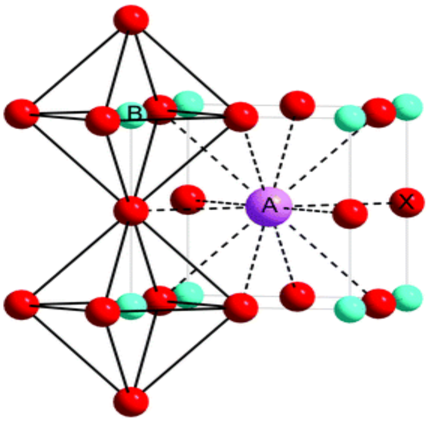

Fig 2. Ideal perovskite structure and the octahedron BX_6.

The stability of cubic perovskites is verified by the tolerance factor of Goldsmith *t*:

$$t = \frac{r_A + r_X}{\sqrt{2}(r_B + r_X)} \tag{14}$$

r_A, r_B *and* r_X are the ionic radius of the A and B cations and the X anion respectively.

Geometrically the ratio between the interatomic distanceD_{A-X} and D_{B-X} is equal to $\sqrt{2}$; while the tolerance factor is 1.

Experimentally, the value of t for cubic perovskites is between 0.8 and 0.9.

Jiang et al. (2006) took 132 perovskite compounds between oxide and hydrides to arrive at a numerical formula of the lattice constant at cubic perovskites. The average error between prediction CP and experimental values is of the order of 0.63%. Other works tried to make some corrections or modifications to the previous models such as Moreira et al. (2007) and Majid et al. (2010).

2-5 Interatomique model of Brik (2011)

Brik (2011) was interested in the cubic perovskite K_2PtCl_6 type. His model is essentially based on the interatomic distances D_{A-X} and D_{M-X} in an A_2MX_6 structure, and the difference in electronegativity of X and M components $\chi_X,\ \chi_M$.

All of these linear dependencies allow it to establish a CP prediction formula for 86 compounds.

3 MODELISATION OF CELL PARAMETER FOR A_2MX_6 PEROVSKITES

3.1 Revised Brik's model

Brik's model is based on the geometric structure of the conventional cell presented in Figure (3). The Wyckoff positions of atoms take the following sites:

- A: 8c (0.25 0.25 0.25)
- M: 4a (0.0 0.0 0.0)
- X: 24 e (0.0 0.0 u)

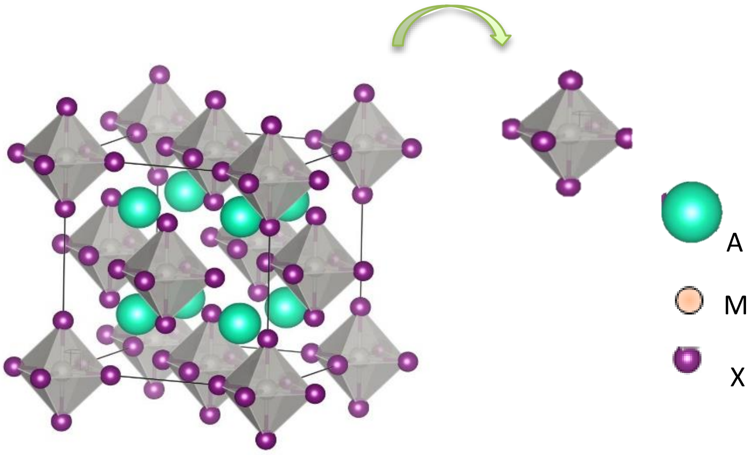

(a) (b)

Fig 3. (a) conventional cell of cubic perovskite A_2MX_6 (b) octahedral BX_6.

The principal quantities in this model are the ionic radius and electronegativity of the constituents. Table (1) shows the properties of the constituents of the studied materials.

Brik proposed a model of CP prediction in a linear form according to the factors: the interatomic distance *d (X-X)* and *d (M-X)* and the electronegativity difference χ_X-χ_M.

Two simple relations between a_{exp} and the interatomic distances are shown in Figures (5-6):

$$a = 1.416.\, d_{X-X} \tag{16}$$

And

$$a = 2.30916\, d\, (M\text{-}X) \tag{17}$$

In these equations, all distances are in A0. It is noted that the shortest and longest inter-ion distances are as follows:

- The distance *d (A - X)* varies from 2.878 Å in K_2NiF_6 to 4.109 Å in Rb_2SnI_6; the distance *d (M-X)* is between 1.677 Å in K_2SiF_6 and 2.847 Å in Rb_2SnI_6; the distance *d (A-M)* increases from 3.511 Å in K_2NiF_6 to 5.032 Å in Rb_2SnI_6.

Moreover, it is easy to obtain that:

$d\,(A\text{-}A) = 2\,d\,(A\text{-}M)$ and $d\,(X\text{-}X) = \sqrt{2}.d\,(M\text{-}X)$ as shown in figure (4)

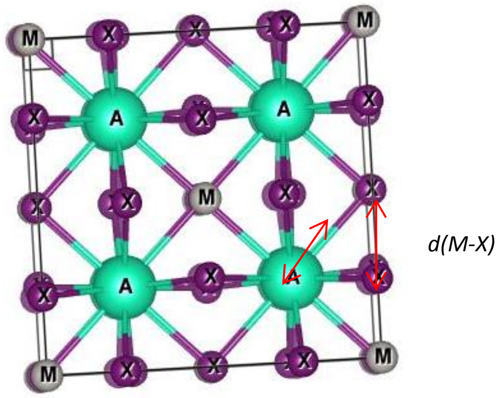

Fig 4. Illustration of interatomic distance d(M-X) and d(X-X).

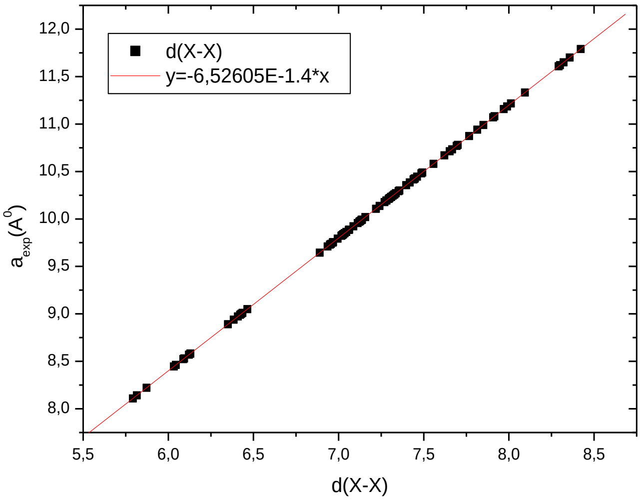

Fig 5. Experimental cell parameter as a function of *d(X-X)*.

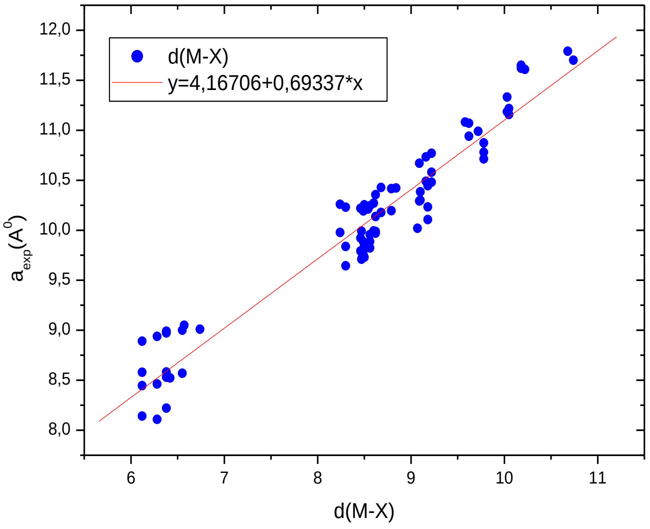

Fig 6. Experimental cell parameter as a function of d_{M-X} , the interatomic distance.

Table 1. Experimental data on lattice constants, ionic radius (Chen et al. 2018), electronegativity (D.R. Lide, 2004) predicted lattice constants, absolute error $(A°)$, and percent relative error for 90 A_2XY_6 compounds.

Compounds	$a_{exp}(A°)$	R_A	R_M	R_X	X_A	XM	Xx	$a_{pred}(A°)$	$\|\Delta a\|(A°)$	Relative error%
Cs_2GeF_6 (Wyckoff & Müller1927)	8,99	1,88	0,53	1,33	0,79	2,01	3,98	8.85321	0,13	1,49
Cs_2MnF_6 (Wyckoff & Müller1927)	8,972	1,88	0,53	1,33	0,79	1,55	3,98	8,89024	0,081	0,91
Cs_2NiF_6 (Hoppe & Hofmann 1977)	8,938	1,88	0,48	1,33	0,79	1,91	3,98	8,8138	0,1241	1,38
Cs_2PdF_6 (Bode et al. 1956)	9	1,88	0,615	1,33	0,79	2,2	3,98	8,92428	0,0757	0,84
Cs_2PtF_6 (Hoppe et al 1952)	9,05	1,88	0,625	1,33	0,79	2,2	3,98	8,93409	0,1159	1,28
Cs_2SiF_6 (Bork et al 1996),	8,89	1,88	0,4	1,33	0,79	1,9	3,98	8,736141	0,1538	1.73
Rb_2CrF_6 (Schütz, 1936)	8,523	1,72	0,55	1,33	0,82	1,66	3,98	8,587397	0,0643	0,75
Rb_2GeF_6 (Hoppe & Klemm 1952)	8,5825	1,72	0,53	1,33	0,82	2,01	3,98	8,541201	0,0412	0,48
K_2HfF_6 (Saalfeld & Guse 1983)	9,01	1,64	0,71	1,33	0,82	1,3	3,98	8,6146357	0,3953643	4,38
K_2MnF_6 (Jiang et al 2006)	8,221	1,64	0,53	1,33	0,82	1,55	3,98	8,4190696	0,1980696	2,40
K_2NiF_6 (Taylor1987)	8,109	1,64	0,48	1,33	0,82	1,91	3,98	8,3426838	0,2336838	2,88
K_2SiF_6 (Hester et al 1993)	8,1419	1,64	0,4	1,33	0,82	1,9	3,98	8,2649615	0,1230615	1,51
Rb_2MnF_6 (Hoppe et al. 1952)	8,531	1,72	0,53	1,33	0,82	1,55	3,98	8,5761296	0,0451296	0,52
Rb_2NiF_6 (Wyckoff & Müller1927)	8,462	1,72	0,48	1,33	0,82	1,91	3,98	8,4997438	0,0377438	0,44
Rb_2PdF_6 (Hoppe & Klemm 1952)	8,57	1,72	0,615	1,33	0,82	2,2	3,98	8,6101618	0,0401618	0,46
Rb_2SiF_6 (Ketelaar et al 1937)	8,446	1,72	0,4	1,33	0,82	1,9	3,98	8,4220215	0,0239785	0,28
Tl_2SiF_6 (Ketelaar et al 1937)	8,58	1,7	0,4	1,33	1,8	1,9	3,98	8,3827565	0,1972435	2,29
Cs_2GeCl_6 (Laubengayer et al 1940)	10,23	1,88	0,53	1,81	0,79	2,01	3,16	10,2063088	0,0236912	0,23
Cs_2IrCl_6 (Coll et al 1990)	10,2119	1,88	0,625	1,81	0,79	2,2	3,16	10,285079	0,073179	0,71
Cs_2MoCl_6 (Hu et al 2005)	10,2121	1,88	0,65	1,81	0,79	2,16	3,16	10,3126417	0,1005417	0,98
Cs_2PbCl_6 (Engel 1935)	10,416	1,88	0,775	1,81	0,79	1,8	3,16	10,462604	0,046604	0,44

Table 1. Experimental data on lattice constants, ionic radius (Chen et al. 2018), electronegativity (D.R. Lide et al. 2004) predicted lattice constants, absolute error ($A°$), and percent relative error for 90 A_2XY_6 compounds *(Continued 1)*

Compounds	$a_{exp}(A°)$	R_A	R_M	R_X	X_A	XM	Xx	$a_{pred}(A°)$	$\|\Delta a\|(A°)$	Relative error%
Cs_2PtCl_6 (Engel 1935)	10,192	1,88	0,625	1,81	0,79	2,2	3,16	10,285079	0,093079	0,91
Cs_2ReCl_6 (Sperka & Maunter,1988)	10,255	1,88	0,63	1,81	0,79	1,9	3,16	10,312763	0,0577631	0,56
Cs_2SeCl_6 (Engel 1935)	10,26	1,88	0,5	1,81	0,79	2,55	3,16	10,135876	0,124124	1,20
Cs_2SnCl_6 (Brill et al 1974)	10,3552	1,88	0,69	1,81	0,79	1,96	3,16	10,367068	0,0118685	0,11
Cs_2TaCl_6 (Yun & Jang, 2007)	10,271	1,88	0,68	1,81	0,79	1,5	3,16	10,3921861	0,1211861	1,17
Cs_2TeCl_6 (Engel 1935)	10,445	1,88	0,97	1,81	0,79	2,1	3,16	10,6311239	0,1861239	1,78
Cs_2TiCl_6 (Hu et al 2005)	10,219	1,88	0,61	1,81	0,79	1,54	3,16	10,3204775	0,1014775	0,99
Cs_2WCl_6 (MÖws et al 1966)	10,245	1,88	0,66	1,81	0,79	1,7	3,16	10,3573797	0,1123797	1,09
Cs_2ZrCl_6 (Engel, 1935),	10,428	1,88	0,72	1,81	0,79	1,33	3,16	10,444335	0,016335	0,15
K_2MnCl_6. (Edwards et al 1962)	9,6445	1,64	0,53	1,81	0,82	1,55	3,16	9,7700566	0,1255566	1,30
K_2MoCl_6 (McCullough, 1936)	9,85	1,64	0,65	1,81	0,82	2,16	3,16	9,8414617	0,0085383	0,08
K_2OsCl_6 (Takazawa et al 1988)	9,729	1,64	0,63	1,81	0,82	2,2	3,16	9,8188041	0,0898041	0,92
K_2PdCl_6 (Williams et al 1973)	9,7097	1,64	0,615	1,81	0,82	2,2	3,16	9,8040888	0,0943888	0,97
K_2PtCl_6. (Grundy & Brown 1970)	9,751	1,64	0,625	1,81	0,82	2,2	3,16	9,813899	0,062899	0,64
K_2ReCl_6 (Deloume et al. 1979)	9,84	1,64	0,63	1,81	0,82	1,9	3,16	9,8415831	0,0015831	0,016
K_2RuCl_6 (Boysen & Hewat, 1978)	9,737	1,64	0,62	1,81	0,82	2,2	3,16	9,8089939	0,0719939	0,73
K_2SnCl_6 (Jongen & Meyer 2004)	9,9877	1,64	0,69	1,81	0,82	1,96	3,16	9,8958885	0,0918115	0,91
K_2TaCl_6 (Elder et al 1967)	9,9935	1,64	0,68	1,81	0,82	1,5	3,16	9,9210061	0,0724939	0,72
K_2TcCl_6 (Bland & Flengas 1961)	9,83	1,64	0,645	1,81	0,82	2,1	3,16	9,8411124	0,0111124	0,11
K_2TiCl_6 (Bland & Flengas 1961)	9,792	1,64	0,61	1,81	0,82	1,54	3,16	9,8492975	0,0572975	0,58
K_2WCl_6 (Xu & Zhao, 2012)	9,8223	1,64	0,66	1,81	0,82	1,7	3,16	9,8861997	0,0638997	0,65
Rb_2MnCl_6 (Lalancette et al 1972)	9,838	1,72	0,53	1,81	0,82	1,55	3,16	9,9271166	0,0891166	0,9058406
Tl_2MoCl_6 (Beck & Hengstmann, 1998)	9,8635	1,7	0,65	1,81	1,8	2,16	3,16	9,9592567	0,0957567	0,9708186
Rb_2NbCl_6 (Henke, 2007)	9,989	1,72	0,68	1,81	0,82	1,6	3,16	10,070473	0,0814731	0,8156281
Rb_2PbCl_6 (Engel, 1935)	10,195	1,72	0,775	1,81	0,82	1,8	3,16	10,148484	0,046516	0,4562628

Table 1. Experimental data on lattice constants, ionic radius (Chen et al. 2018), electronegativity (D.R. Lide et al. 2004) predicted lattice constants, absolute error $(A°)$, and percent relative error for 90 A_2XY_6 compounds *(Continued 2)*

Compounds	$a_{exp}(A°)$	R_A	R_M	R_X	X_A	XM	Xx	$a_{pred}(A°)$	$\|\Delta a\|(A°)$	Relative error%
Rb_2PdCl_6 (Ketelaar, 1935)	9,99	1,72	0,615	1,81	0,82	2,2	3,16	9,9611488	0,0288512	0,2888008
Rb_2PtCl_6 (Engel, 1935)	9,884	1,72	0,625	1,81	0,82	2,2	3,16	9,970959	0,086959	0,8797956
Tl_2PtCl_6. (Engel, 1935)	9,755	1,7	0,625	1,81	1,8	2,2	3,16	9,931694	0,176694	1,8113172
Rb_2SeCl_6 (Engel, 1935),	9,978	1,72	0,5	1,81	0,82	2,55	3,16	9,821756	0,156244	1,56588495
Rb_2SnCl_6 (Abriel et al 1987)	10,137	1,72	0,69	1,81	0,82	1,96	3,16	10,052948	0,0840515	0,82915557
Rb_2TeCl_6. (Collins & Webster, 1974)	10,233	1,72	0,97	1,81	0,82	2,1	3,16	10,317003	0,0840039	0,82091176
Rb_2TiCl_6 (Wang et al 2002)	9,922	1,72	0,61	1,81	0,82	1,54	3,16	10,006357	0,0843575	0,85020661
Rb_2WCl_6 (Zheng et al 1998)	9,957	1,72	0,66	1,81	0,82	1,7	3,16	10,043259	0,0862597	0,86632219
Rb_2ZrCl_6 (Magette & Fuger, 1977)	10,178	1,72	0,72	1,81	0,82	1,33	3,16	10,130215	0,047785	0,46949302
Tl_2SnCl_6 (Bagnall et al 1956)	9,97	1,7	0,69	1,81	1,8	1,96	3,16	10,013683	0,0436835	0,43814945
Tl_2TeCl_6 (Ferrari & Coghi, 1941)	10,107	1,7	0,97	1,81	1,8	2,1	3,16	10,277738	0,1707389	1,68931335
Tl_2WCl_6 (Ketelaar et al 1937)	9,8873	1,7	0,66	1,81	1,8	1,7	3,16	10,003994	0,1166947	1,1802484
Cs_2NpBr_6 (Vdovenko et al 1973)	11,082	1,88	0,87	1,96	0,79	1,3	2,96	11,0202204	0,0617796	0,55747699
Cs_2PoBr_6 (Zheng et al 1997b)	10,99	1,88	0,94	1,96	0,79	2	2,96	11,035740	0,0457408	0,41620382
Cs_2PtBr_6 (Abriel & White 1990)	10,67	1,88	0,625	1,96	0,79	2,2	2,96	10,711533	0,0415335	0,38925492
Cs_2SnBr_6 (Abriel, 1984)	10,77	1,88	0,69	1,96	0,79	1,96	2,96	10,793523	0,023523	0,21841226
Cs_2TeBr_6 (Stoll et al 1926)	10,873	1,88	0,97	1,96	0,79	2,1	2,96	11,057578	0,1845784	1,69758484
Cs_2UBr_6 (Abriel, 1984)	11,07	1,88	0,89	1,96	0,79	1,7	2,96	11,009468	0,0605312	0,54680397
Cs_2WBr_6 (Zheng et al 1997b)	10,733	1,88	0,66	1,96	0,79	1,7	2,96	10,783834	0,0508342	0,47362527
K_2OsBr_6 (Takazawa et al 1988)	10,3	1,64	0,63	1,96	0,82	2,2	2,96	10,245258	0,0547414	0,5314699
K_2PtBr_6 (Deloume et al 1979)	10,293	1,64	0,625	1,96	0,82	2,2	2,96	10,240353	0,0526465	0,51147867
K_2ReBr_6 (Deloume et al 1979)	10,385	1,64	0,63	1,96	0,82	1,9	2,96	10,268037	0,1169624	1,12626288
K_2SeBr_6 (Schupp et al 2000)	10,4224	1,64	0,5	1,96	0,82	2,55	2,96	10,091150	0,3312495	3,17824589
K_2SnBr_6 (Abriel, 1984)	10,48	1,64	0,69	1,96	0,82	1,96	2,96	10,322343	0,157657	1,50436069
K_2TeBr_6 (Stoll et al 1926)	10,78	1,64	0,97	1,96	0,82	2,1	2,96	10,586398	0,1936016	1,79593321

Table 1. Experimental data on lattice constants, ionic radius (Chen et al. 2018), electronegativity (D.R. Lide et al. 2004) predicted lattice constants, absolute error $(A°)$, and percent relative error for 90 A_2XY_6 compounds *(Continued 3)*

Compounds	$a_{exp}(A°)$	R_A	R_M	R_X	X_A	XM	Xx	$a_{pred}(A°)$	$\|\Delta a\|(A°)$	Relative error%
Rb_2PdBr_6 (Abriel, 1984)	10,02	1,72	0,615	1,96	0,82	2,2	2,96	10,387603	0,3676033	3,66869561
Rb_2SnBr_6 (Zheng et al 1997a)	10,58	1,72	0,69	1,96	0,82	1,96	2,96	10,479403	0,100597	0,95082231
Rb_2TeBr_6 (Schupp et al 2000)	10,713	1,72	0,97	1,96	0,82	2,1	2,96	10,743458	0,0304584	0,28431252
Rb_2UBr_6 (Thiele et al 1983)	10,94	1,72	0,89	1,96	0,82	1,7	2,96	10,695348	0,2446512	2,23629982
Rb_2WBr_6 (Werker, 1939)	10,489	1,72	0,66	1,96	0,82	1,7	2,96	10,469714	0,0192858	0,18386691
Rb_2PdI_6 (Sinram et al 1982)	11,185	1,72	0,615	2,2	0,82	2,2	2,66	11,071449	0,1135509	1,01520697
Rb_2PtI_6 (Schupp et al 2000)	11,217	1,72	0,625	2,2	0,82	2,2	2,66	11,081259	0,1357407	1,21013373
Rb_2SnI_6 (Zheng et al 1997a)	11,62	1,72	0,69	2,2	0,82	1,96	2,66	11,163248	0,4567512	3,93073322
Cs_2HfI_6 (Sinram et al 1982)	11,609	1,88	0,71	2,2	0,79	1,3	2,66	11,547103	0,061897	0,53318115
Cs_2PdI_6 (Schupp et al 2000)	11,332	1,88	0,615	2,2	0,79	2,2	2,66	11,385569	0,0535691	0,47272414
Cs_2PoI_6 (Bagnall et al 1955)	11,79	1,88	0,94	2,2	0,79	2	2,66	11,719586	0,0704134	0,59722986
Cs_2PtI_6 (Thiele et al 1983)	11,158	1,88	0,625	2,2	0,79	2,2	2,66	11,395379	0,2373793	2,12743592
Cs_2SnI_6 (Werker, 1939)	11,65	1,88	0,69	2,2	0,79	1,96	2,66	11,477368	0,1726312	1,48181288
Cs_2TeI_6 (Thiele et al 1983)	11,7	1,88	0,97	2,2	0,79	2,1	2,66	11,741424	0,0414242	0,35405299
Cs_2TiBr_6 (Smok et al 2002)	10,92	1,88	0,61	1,96	1,052227	0,64	9,96	11,346779	0,426779	3,9082326
Cs_2Til_6. (Smok et al 2002)	11,67	1,88	0,61	2,2	1,022505	0,43	9,96	12,069349	0,3993491	3,42201457
Cs_2HfCl_6 (Nagorny, 2021)	10,42	1,88	0,71	1,81	1,031187	0,34	10,36	11,056391	0,6363915	6,10740403
Cs2HfBr6 (Yao et al 2022)	10,83	1,88	0,71	1,96	1,012818	0,15	10,36	11,512458	0,6824587	6,30155771

Although ionic radius is a primary factor governing the structure of the crystal lattice, ionic radius alone can't adequately describe the parameter variation of the lattice in this series.

To properly manage this situation and similar situations, the electronegativity of the corresponding chemical elements should also be considered.

Because the cell parameter a represents a balance between effective ionic radii and their electronegativity, the CP in this model has been expressed as a linear function of the following variables:

Two sums of ionic rays $(R_A + R_X)$, $(R_M + R_X)$ and electronegativity difference $(\chi_X\text{-}\chi_M)$ The regression by the least square method resulted in the following linear function:

$$a = 1.96325.\ (R_A + R_X)+0.98102.\ (R_M + R_X)+0.07593.\ (\chi_X\text{-}\chi_M)+0.57901 \tag{18}$$

On our part, we have generalized the formula of brik by adding 4 new materials recently synthesized (S. Nagorny et al. 2021) The application of this formula based on 90 materials allowed the prediction of CP a with a relative error of 1.22%. The results of this prediction are presented in Table (1).

Figure (7) shows the different families studied separately: Florides A_2MF_6, Chlorides A_2MCl_6, Brorures A_2MBr_6, and Iodies A_2MI_6.

The interpretation of the prediction results leads us to the following remarks:

The big error value on fluorides K2HfF6 is: 4.38%

The big error values to the family bromures are:

- Cs_2HfBr_6: 6.30%
- Cs_2TiBr_6: 3.90%
- Rb_2PdBr6: 3.66%
- K2SeBr6: 3.17%

The large error on chloride is 6.10% for Cs_2HfCl_6.

The big error values of the iodides family are:

- Rb2SnI6: 3.93%
- Cs2TiI6: 3.422%.

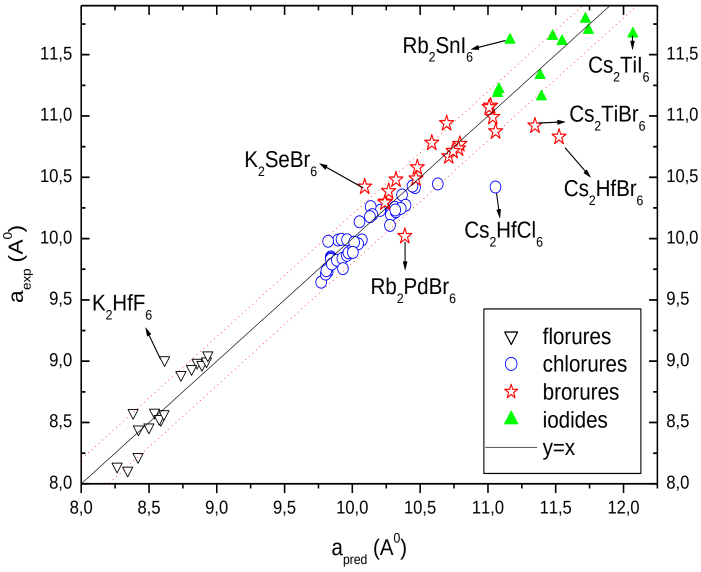

Fig 7. a_{pred} as a function of a_{exp} for different perovskites series.

3.2 New Modelisation using Jiang's Model

Jiang's model (L.Q. Jiang et al. 2008) was applied for perovskites ABX_3 of cubic structure type pm3m. In this work, we will apply this model for materials A_2MX_6. The input parameters of this model are:

- The ionic radius of the constituents and the tolerance factor of Goldsmith *t*.
- Tolerance factor values for A_2MX_6 are presented in Figure 8.
- We plot the curve that shows the variation of a_{exp}-4 (r_M + r_X) as a function of t as shown in Fig. (9)

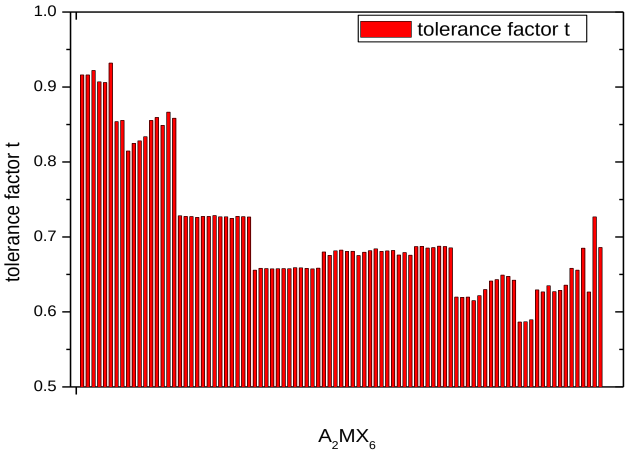

Fig 8. Tolerance factor t values of 90 A_2MX_6 compound.

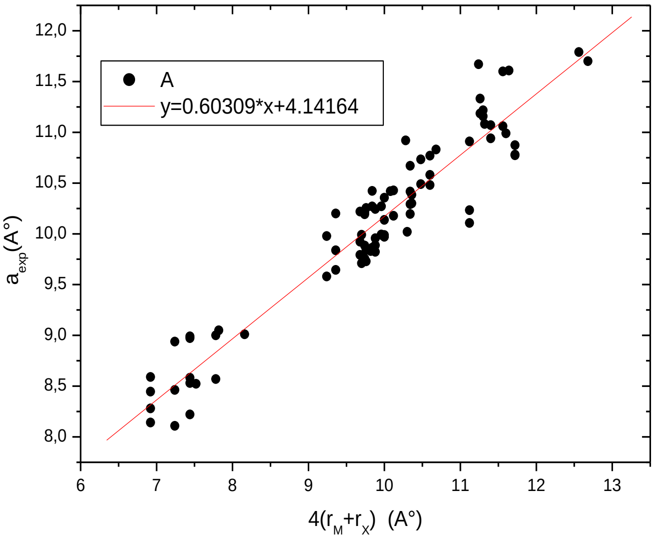

Fig 9. Linear relationship between a_{exp} and $4(r_M+r_X)$.

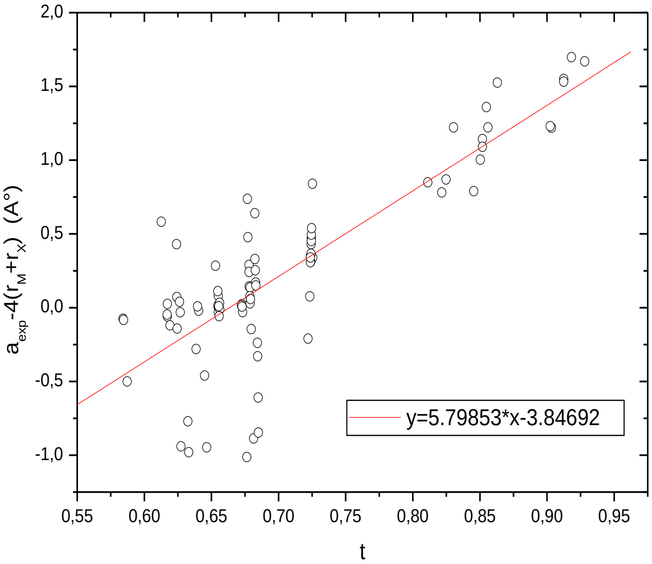

Fig 10. Variation of a_{exp}-$4(r_M + r_X)$ as tolerance factor t.

From linear regression LR of these inputs, we find:

$$a_{exp}\text{-}4(r_M + r_X)\text{=}5.798\text{*}t\ \text{-}3.84692 \qquad (18)$$

and the relation obtained from Fig. 9 is

$$a_{exp}\ \text{=}0.604\text{*}(r_M\text{+}r_X)\ \text{+}4.14 \qquad (19)$$

So

$$2a_{exp}\text{=}\ (1.6)\text{*}4(r_M + r_X)\ \text{+}5.798\text{*}t\text{+}4.14\text{-}3.84 \qquad (20)$$

Which result

$$a_{exp}\text{=}3.2\text{*}\ (r_M + r_X)\text{+}2.899t\text{-}0.15 \qquad (21)$$

A new prediction formula is obtained as:

$$a_{pred}\text{=}3.2\text{*}\ (r_M + r_X)\text{+}2.899t\text{-}0.15 \qquad (22)$$

This formula is used to predict the CP of studied materials and a comparison between prediction and experimental values of CP with an average error of 1.13%.

4. CONCLUSION

The prediction of the CP of the different crystalline structures makes the object of several searches (L.Q. Jiang et al. 2006; M.W. Lufaso 2001; A. Kojima et al. 2009; W. S. Yang et al. 2017; C. Kalaiselvi et al. 2018; L. Chonghe et al. 2003). We presented in this paper two semi-empirical models: the model of Brik et al. (2011) and the model of Jiang et al. (2006).

The application of the two models on a set of 90 compounds of types A_2 MX_6 and comparison of the prediction results using these models gives a relative error of the order of:

- 1.22% for Brik's model.
- 1.13% for Jiang's model.

Reformulation of Jiang's model for A_2 MX_6 perovskites gives a new equation of prediction with less error than Brik's model. This prediction can be useful for the estimation of physical properties of new compounds as Cs_2ZrI_6 that we predict its CP to be a=9.13A°.

REFERENCES

Abriel, W. (1984). Polymorphism and phase transitions of K2TeBr6: A single crystal investigation of the high temperature phases (383–463 K). *Materials research bulletin*, *19*(3), 313-318.. https://doi.org/10.1016/0025-5408(84)90172-7.

Abriel, W. & Du Bois, A. (1989). Structure of bis (tetraphenylarsonium) hexabromotellurate (IV). *Acta Crystallographica Section C: Crystal Structure Communications*, *45*(12), 2002-2003. https://doi.org/10.1107/S0108270189008826.

Abriel, W. & Ihringer, J. (1984). Crystal structures and phase transition of Rb2TeBr6 (300-12.5 K). *Journal of Solid State Chemistry*, *52*(3), 274-280. https://doi.org/10.1016/0022-4596(84)90010-0.

Abriel, W. & White, M. A. (1990). The phase transitions of ferroelastic K2SeBr6: A calorimetric and x-ray diffraction study. *The Journal of Chemical Physics*, *93*(11), 8321-8327. https://doi.org/10.1063/1.459315.

Bagnall, K. W., d'Eye, R. W. M. & Freeman, J. H. (1955). The polonium halides. Part II. bromides. *Journal of the Chemical Society (Resumed),* 3959-3963. https://doi.org/10.1039/JR9550003959.

Bagnall, K. W., D'Eye, R. W. M. & Freeman, J. H. (1956). 657. The polonium halides. Part III. Polonium tetraiodide. *Journal of the Chemical Society (Resumed),* 3385-3389. https://doi.org/10.1039/JR9560003385.

Beck, J. & Hengstmann, M. (1998). Über Thallium (I)-chlorooxomolybdate: Synthese und Kristallstrukturen von Tl [MoOCl4 (NCCH3)], Tl [Mo2O2Cl7] und Tl2 [Mo4O4Cl14] und die Struktur von Tl2 [MoCl6]. *Zeitschrift für anorganische und allgemeine Chemie*, *624*(12), 1943-1950. https://doi.org/10.1002/(SICI)1521-3749(1998120)624:12%3C1943::AID-ZAAC1943%3E3.0.CO;2-6

Bland, J. A. & Flengas, S. N. (1961). The Crystal Structure of K2TiCl6. *Canadian Journal of Physics*, *39*(6), 941-944.https://doi.org/10.1139/p61-100.

Bode, H. & Voss, E. (1956). Über Strukturen von Fluorokomplexen mit vierwertigem Nickel und Chrom. *Zeitschrift für anorganische und allgemeine Chemie*, *286*(3-4), 136-141. https://doi.org/10.1002/zaac.19562860304.

Bork, M. & Hoppe, R. (1996). Der erste Vertreter des K2PtCl6-Typs bei Fluoriden A2 [PtF6]: β-Cs2 [PtF6]. *Zeitschrift für anorganische und allgemeine Chemie*, *622*(3), 417-424. https://doi.org/10.1002/zaac.19966220307.

Boysen, H. A. N. S. & Hewat, A. W. (1978). A neutron powder investigation of the structural changes in K2SnCl6. *Acta Crystallographica Section B: Structural Crystallography and Crystal Chemistry*, *34*(5), 1412-1418. https://doi.org/10.1107/S0567740878005816.

Brill, T. B., Gearhart, R. C. & Welsh, W. A. (1974). Crystal structures of M2SnCl6 salts. An analysis of the "crystal field effect" in their nuclear quadrupole resonance and vibrational spectra. *Journal of Magnetic Resonance (1969)*, *13*(1), 27-37. https://doi.org/10.1016/0022-2364(74)90101-2.

Brik, M. G. & Kityk, I. V. (2011). Modeling of lattice constant and their relations with ionic radii and electronegativity of constituting ions of A2XY6 cubic crystals (A= K, Cs, Rb, Tl; X= tetravalent cation, Y= F, Cl, Br, I). *Journal of Physics and Chemistry of Solids*, *72*(11), 1256-1260. https://doi.org/10.1016/j.jpcs.2011.07.016.

Chen, M., Ju, M. G., Carl, A. D., Zong, Y., Grimm, R. L., Gu, J., ... & Padture, N. P. (2018). Cesium titanium (IV) bromide thin films based stable lead-free perovskite solar cells. *Joule*, *2*(3), 558-570.https://www.cell.com/joule/fulltext/S2542-4351(18)30037-0.

Chonghe, L., Yihao, T., Yingzhi, Z., Chunmei, W. & Ping, W. (2003). Prediction of lattice constant in perovskites of GdFeO3 structure. *Journal of Physics and Chemistry of Solids*, *64*(11), 2147-2156. https://doi.org/10.1016/S0022-3697(03)00209-9.

Coll, R. K., Fergusson, S. E., Penfold, B. R., Rankin, D. A. & Robinson, W. T. (1990). The preparative and structural chemistries of hexahalogeno and trichlorostannato complexes of iridium. *Inorganica chimica acta*, *177*(1), 107-114. https://doi.org/10.1016/S0020-1693(00)91918-2.

Deloume, J. P., Faure, R. & Thomas-David, G. (1979). Nouvelle détermination de la structure cristalline du μ-oxo-bis [pentachlororuthénate (IV)] de potassium, K4 [Ru2Cl10O] et affinement de la structure de l'hexachlororuthénate de potassium K2 [RuCl6]. *Acta Crystallographica Section B: Structural Crystallography and Crystal Chemistry*, *35*(3), 558-561.https://doi.org/10.1107/S0567740879004143.

Edwards, A. J., Peacock, R. D. & Said, A. (1962). 894. Complex chlorides and bromides of quadrivalent molybdenum. *Journal of the Chemical Society (Resumed)*, 4643-4648. https://doi.org/10.1039/JR9620004643.

Elder, M., Fergusson, J. E., Gainsford, G. J., Hickford, J. H. & Penfold, B. R. (1967). Potassium pentachlorohydroxytechnetate (IV). *Journal of the Chemical Society A: Inorganic, Physical, Theoretical*, 1423-1425. https://doi.org/10.1039/J19670001423.

Engel, G. (1935). Die kristallstrukturen einiger hexachlorokomplexsalze. *Zeitschrift für Kristallographie. Crystalline Materials*, *90*(1-6), 341-373. https://doi.org/10.1524/zkri.1935.90.1.341.

Feng, L. M., Jiang, L. Q., Zhu, M., Liu, H. B., Zhou, X. & Li, C. H. (2008). Formability of ABO3 cubic perovskites. *Journal of Physics and Chemistry of Solids*, *69*(4), 967-974. https://doi.org/10.1016/j.jpcs.2007.11.007.

Ferrari, A. & Coghi, L. (1941). On the existence of hexahalogenoaurates. *Gazz. Chim. Ital*, *71*, 440-441 https://doi.org/10.1021/ic50081a044.

Fukunaga, O. & Fujita, T. (1973). The relation between ionic radii and cell volumes in the perovskite compounds. *Journal of Solid State Chemistry*, *8*(4), 331-338. https://doi.org/10.1016/S0022-4596(73)80030-1.

Geiger, E. (1926). *Ueber die Konstitution der Hochpolymeren* (Doctoral dissertation, ETH Zurich). https://doi.org/10.1016/j.jpcs.2011.07.016.

Grundy, H. D. & Brown, I. D. (1970). A refinement of the crystal structures of K2ReCl6, K2ReBr6, and K2PtBr6. *Canadian Journal of Chemistry*, *48*(7), 1151-1154. https://doi.org/10.1139/v70-189.

Henke, H. (2007). The significance of the Jahn-Teller effect for the phase transitions of K2NbCl6 and Rb2NbCl6. *Zeitschrift für Kristallographie*, *222*(9), 477-486. https://doi.org/10.1524/zkri.2007.222.9.477.

Hester, J. R., Maslen, E. N., Spadaccini, N., Ishizawa, N. & Satow, Y. (1993). Accurate synchrotron radiation Δρ maps for K2SiF6 and K2PdCl6. *Acta Crystallographica Section B: Structural Science*, *49*(6), 967-973. https://doi.org/10.1107/S0108768193005725.

Hoppe, R. & Hofmann, B. (1977). News on K2(MnF6), Rb2/(MnF6) and Cs2/(MnF6). *Z. Anorg. Allg. Chem*, *436*. 65-74. https://inis.iaea.org/records/5ns1n-g4r88.

Hoppe, R. & Klemm, W. (1952). Über Fluorokomplexe des Palladiums und des Goldes. *Zeitschrift für anorganische und allgemeine Chemie*, *268*(4-6), 364-371. https://doi.org/10.1002/zaac.19522680415.

Hu, B., Wang, P., Xiao, Y. & Song, L. P. (2005). Crystal structure of dicesium hexachloromolybdate (IV), Cs2 [MoCl6]. *Zeitschrift für Kristallographie-New Crystal Structures*, *220*(1-4), 318-318. https://doi.org/10.1524/ncrs.2005.220.14.318.

Jiang, L. Q., Guo, J. K., Liu, H. B., Zhu, M., Zhou, X., Wu, P. & Li, C. H. (2006). Prediction of lattice constant in cubic perovskites. *Journal of Physics and Chemistry of Solids*, *67*(7), 1531-1536. https://doi.org/10.1016/j.jpcs.2006.02.004.

Jongen, L. & Meyer, G. (2004). Dipotassium hexachlorotantalate (IV), K2TaCl6. *Acta Crystallographica Section E: Structure Reports Online*, *60*(8), 91-92. https://doi.org/10.1107/S1600536804016198.

Kalaiselvi, C. R., Muthukumarasamy, N., Velauthapillai, D., Kang, M. & Senthil, T. S. (2018). Importance of halide perovskites for next generation solar cells–a review. *Materials Letters*, *219*, 198-200. https://doi.org/10.1016/j.matlet.2018.02.089.

Ketelaar, J. A. A. (1935). Die Kristallstruktur von K-, Rb-, Cs-und Tl-Silicofluorid und von LiMnO4-3H2O. Zeitschrift für Kristallographie-Crystalline Materials, 92(1-6), 155-156. https://doi.org/10.1524/zkri.1935.92.1.155.

Ketelaar, J. A. A., Rietdijk, A. A. & Van Staveren, C. H. (1937). Die Kristallstruktur von Ammonium-, Kalium-, Rubidium-und Cäsiumstannibromid. *Recueil des Travaux Chimiques des Pays-Bas*, *56*(9), 907-908. https://doi.org/10.1002/recl.19370560913.

Kojima, A., Teshima, K., Shirai, Y. & Miyasaka, T. (2009). Organometal halide perovskites as visible-light sensitizers for photovoltaic cells. *Journal of the American Chemical Society*, *131*(17), 6050-6051. https://pubs.acs.org/doi/10.1021/ja809598r.

Kumar, A., Verma, A. S. & Bhardwaj, S. R. (2008). Prediction of formability in perovskite-type oxides. The Open Applied Physics Journal, 1:11-19. http://dx.doi.org/10.2174/1874183500801010011.

Lalancette, R. A., Elliott, N. & Bernal, I. (1972). Crystal structures and magnetic properties of a 2 mncl 6 salts (a= nh4+, k+ and rb+). *Journal of Crystal and Molecular Structure*, *2*, 143-149. https://doi.org/10.1007/BF01464795.

Laubengayer, A. W., Billings, O. B. & Newkirk, A. E. (1940). Chlorogermanic acid and the chlorogermanates. Properties and crystal structure of cesium hexachlorogermanate. *Journal of the American Chemical Society*, *62*(3), 546-548. https://pubs.acs.org/doi/pdf/10.1021/ja01860a027.

Lee, J. W. & Cho, J. S. (2010). Effective lane detection and tracking method using statistical modeling of color and lane edge-orientation in Advanced Information Sciences and Service Sciences. DOI:10.4156/aiss.vol2.issue3.16Source:DBLP.

Lide, D. R. (Ed.). (2004). *CRC handbook of chemistry and physics* (Vol. 85). CRCpress. https://journals.iucr.org/paper?pii=S0567739476001551.

Lufaso, M. W. (2002). *Perovskite synthesis and analysis using structure prediction diagnostic software* (Doctoral dissertation, The Ohio State University). https://www.proquest.com/openview/837fefb7f3c7154a3c068d24795383e5/1?pq-origsite=gscholar&cbl=18750&diss=y.

Lufaso, M. W. & Woodward, P. M. (2001). Prediction of the crystal structures of perovskites using the software program SPuDS. *Acta Crystallographica Section B: Structural Science*, *57*(6), 725-738. https://doi.org/10.1107/S0108768101015282.

Majid, A., Khan, A. & Choi, T. S. (2011). Predicting lattice constant of complex cubic perovskites using computational intelligence. *Computational Materials Science*, *50*(6), 1879-1888. https://doi.org/10.1016/j.commatsci.2011.01.035.

Magette, M. & Fuger, J. (1977). Preparation, crystal structure and enthalpy of formation of dicaesium hexabromoneptunate. Inorganic and Nuclear Chemistry Letters, 13(10), 529-536. https://doi.org/10.1016/0020-1650(77)80023-8.

Maughan, A. E., Ganose, A. M., Bordelon, M. M., Miller, E. M., Scanlon, D. O. & Neilson, J. R. (2016). Defect tolerance to intolerance in the vacancy-ordered double perovskite semiconductors Cs2SnI6 and Cs2TeI6. *Journal of the American Chemical Society*, *138*(27), 8453-8464. https://pubs.acs.org/doi/10.1021/jacs.6b03207.

McCullough, J. D. (1936). Kristallgeometrie Kristallphys Kristallchem. *Z Kristallogr*, *94*, 143. https://doi.org/10.1524/zkri.1936.94.1.143.

Moreira, R. L. & Dias, A. (2007). Comment on "Prediction of lattice constant in cubic perovskites". *Journal of Physics and Chemistry of Solids*, *68*(8), 1617-1622. https://doi.org/10.1016/j.jpcs.2007.03.050.

Mows, P.C. (1966). The Crystal Structure, Visible, and Ultraviolet Spectra of Potassium Hexachloromanganate (IV). Inorganic Chemistry, 5, 5-8. https://doi.org/10.1021/ic50035a002.

Nagorny, S. (2021). Novel Cs_2HfCl_6 Crystal Scintillator: Recent Progress and Perspectives, *Physics* 2021, *3*(2), 320-351. https://doi.org/10.3390/physics3020023.

Saalfeld, H. & Guse, W. (1983). The polymorphism of K2HfF6. https://pascal-francis.inist.fr/vibad/index.php?action=getRecordDetail&idt=PASCAL83X0323830.

Schüpp, B., Heines, P. & Keller, H. L. (2000). Zwei neue Iodopalladate mit gleicher Summenformel: Rb2PdI4· I2–ein neuer Strukturtyp mit eingelagerten I2-Molekülen–und Rb2PdI6. *Zeitschrift für anorganische und allgemeine Chemie*, *626*(1), 202-207. https://doi.org/10.1002/(SICI)1521-3749(200001)626:1<202::AID-ZAAC202>3.0.CO;2-7.

Schüpp, B., Heines, P., Savin, A. & Keller, H. L. (2000). Crystal Structures and Pressure-Induced Redox Reaction of Cs2PdI4I2 to Cs2PdI6. *Inorganic Chemistry*, *39*(4), 732-735. https://doi.org/10.1021/ic990670.

Schütz, W. (1936). Die kristallchemische Verwandtschaft zwischen Germanium und Silicium. *Zeitschrift für Physikalische Chemie*, *31*(1), 292- 308. https://doi.org/10.1152/physrev.1957.37.4.475.

Shannon, R. D. (1976). Revised effective ionic radii and systematic studies of interatomic distances in halides and chalcogenides. *Foundations of Crystallography*, *32*(5), 751-767. https://doi.org/10.1107/S0567739476001551.

Sinram, D., Brendel, C. & Krebs, B. (1982). Hexa-iodoanions of titanium, zirconium, hafnium, palladium and platinum: preparation, properties and crystal structures of the cesium salts. Inorganica Chimica Acta, 64, L131-L132. 10.1016/s0020-1693(00)90301-3.

Smith, P. J., White, R. F. M. & Smith, L. (1972). A 119Sn NMR and Mössbauer study of some di-and tri-alkyltin (IV) alkoxides. *Journal of Organometallic Chemistry*, *40*(2), 341-353. https://doi.org/10.1080/00958970500240649.

Smok, P., Kityk, I. V., Plucinski, K. J. & Berdowski, J. (2002). Origin of giant anisotropy in synthesized Ba pentaborates. *Physical Review B*, *65*(20), 205103. https://doi.org/10.1103/PhysRevB.65.205103.

Sperka, G. & Maunter, F. A. (1988). Crystal growth and structure of Cs2ReCl6. *Crystal research and technology*, *23*(7), K109-K111. https://doi.org/10.1515/znb-1983-0802.

Stoll, P. (1926). *Raumgitter von Komplexsalzen* (Doctoral dissertation, ETH Zurich).

Takazawa, H., Ohba, S. & Saito, Y. (1988). Electron-density distribution in crystals of dipotassium tetrachloropalladate (II) and dipotassium hexachloropalladate (IV), K2 [PdCl4] and K2 [PdCl6] at 120 K. Acta Crystallographica Section B: Structural Science, 44(6), 580-585. https://doi.org/10.1107/S0108768188010031.

Taylor, J. C. (1987). A comparison of profile decomposition and Rietveld methods for structural refinement with powder diffraction data. *Zeitschrift für Kristallographie-Crystalline Materials*, *181*(1-4), 151-160. https://doi.org/10.1524/zkri.1987.181.14.151.

Thiele, G., Mrozek, C., Kammerer, D. & Wittmann, K. (1983). On hexaiodoplatinates (iv) m2pti6 (m= k, rb, cs, nh4, tl)-preparation, properties and structural data. Zeitschrift Fur Naturforschung Section Ba Journal of Chemical Sciences, *38*(8), 905-910. https://doi.org/10.1515/znb-1983-0802.

Vdovenko, V. M., Kozhina, I. I., Suglobova, I. G. & Chirkst, D. E. (1973). Complexing in uranium halogenide-alkali metal halogenide systems. Radiokhimiya, *15*(1), 54-57 https://inis.iaea.org/search/search.aspx?orig_q=RN:407345957.

Collins, P. H. & Webster, M. (1974). Crystal and molecular structure of tetraphenylarsonium aquotetrachlorohydroxotellurate (IV). J. Chem. Soc., Dalton Trans. (15). https://doi.org/10.1039/DT9740001545.

Wei, D. Y., Lin, J. L. & Zheng, Y. Q. (2002). Note: The crystal structure of Tris (nitrate-O, O') bis (1, 10-phenanthroline-N, N') terbium (III). Journal of Coordination Chemistry, *55*(11), 1259-1262.

Werker, W. (1939). Die krystallstruktur des Rb2SnJ6 und Cs2SnJ6. *Recueil des Travaux Chimiques des Pays-Bas*, *58*(3), 257-258. https://doi.org/10.1002/recl.19390580309.

Williams, R. J., Dillin, D. R. & Milligan, W. O. (1973). Structure refinement of potassium chloroplatinate by powder and single-crystal methods. *Acta Crystallographica Section B: Structural Crystallography and Crystal Chemistry*, *29*(7), 1369-1372. https://doi.org/10.1107/S0108768188010031.

Wyckoff, R. W. & Müller, J. H. (1927). The crystal structure of cesium fluogermanate. *Am J Sci*, *76*, 347-352. https://ajsonline.org/cgi/doi/10.2475/ajs.s5-16.94.349.

Xu, R., Ye, Y. & Zhao, W. (Eds.). (2012). Introduction to natural products chemistry (pp. 101-118). Science Press. DOI: 10.1524/zkri.217.3.301.16032.

Yang, W. S., Park, B. W., Jung, E. H., Jeon, N. J., Kim, Y. C., Lee, D. U., ... & Seok, S. I. (2017). Iodide management in formamidinium-lead-halide–based perovskite layers for efficient solar cells. *Science*, *356*(6345), 1376-1379. https://doi.org/10.1126/science.aan2301.

Yao, J., Kong, J., Shi, W. & Lu, C. (2022). The insolubility problem of organic hole-transport materials solved by solvothermal technology: toward solution-processable perovskite solar cells. *ACS Applied Materials & Interfaces*, *14*(5), 7493-7503. https://doi.org/10.1021/acsami.1c24035.

Yun, H. & Jang, G. J. (2007). Dicaesium hexachlorotantalate (IV), Cs2TaCl6. *Acta Crystallographica Section E: Structure Reports Online*, *63*(1), i22-i23. https://doi.org/10.1107/S1600536806054754.

Zheng, Y. Q., Nuss, J. & Schnering, H. V. (1998). Crystal structure of dithallium hexachlorotungstate (IV), Tl2 [WCl6]. *Zeitschrift für Kristallographie-New Crystal Structures*, *213*(1-4), 500-500 https://doi.org/10.1524/ncrs.1998.213.14.500.

Zheng, Y. Q., Peters, K. & Schnering, H. V. (1997a). Crystal structure of dirubidium hexabromotungstate (IV), Rb2WBr6. *Zeitschrift für Kristallographie-Crystalline Materials*, *212*(1), 53-53. https://doi.org/10.1515/zkri-1997-2120117.

Zheng, Y. Q., Peters, K. & Schnering, H. V. (1997b). Crystal structure of dicesium hexabromotungstate (IV), Cs2WBr6. *Zeitschrift für Kristallographie-Crystalline Materials*, *212*(1), 55-55. https://doi.org/10.1515/zkri-1997-2120119.

Zheng, Y. Q., Sun, J. & Wang, Y. F. (2005). The first suberate-bridged lanthanide coordination polymer: synthesis, crystal structure and properties of La2 (H2O) 2L3 (H2L= HOOC (CH2) 6COOH). *Journal of Coordination Chemistry*, *58*(17), 1551-1559. https://doi.org/10.1016/S0022-328X(00)93372-2.